Schematic View of Diagnostic Set installed at the DPF-1000U Device Chamber

Standard Arrangement
(Most frequently used across many experimental campaigns)

Fully configured for the first time in September, 2015

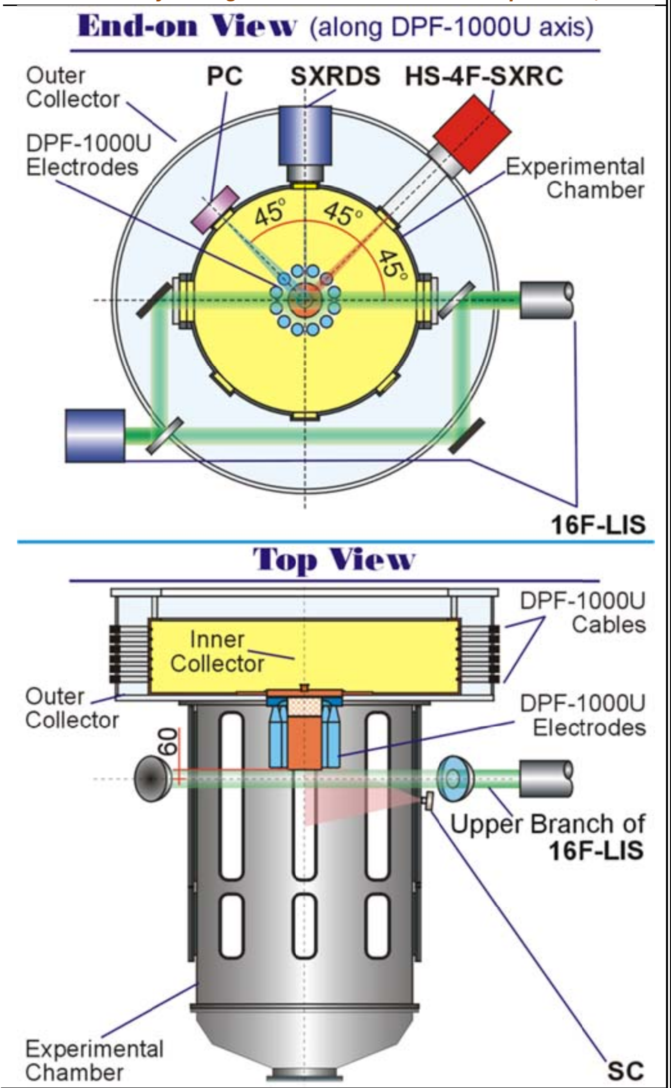

Partially reconfigured and expanded arrangement for plasma jet formation & flow studies

Applied for the first time in June, 2017

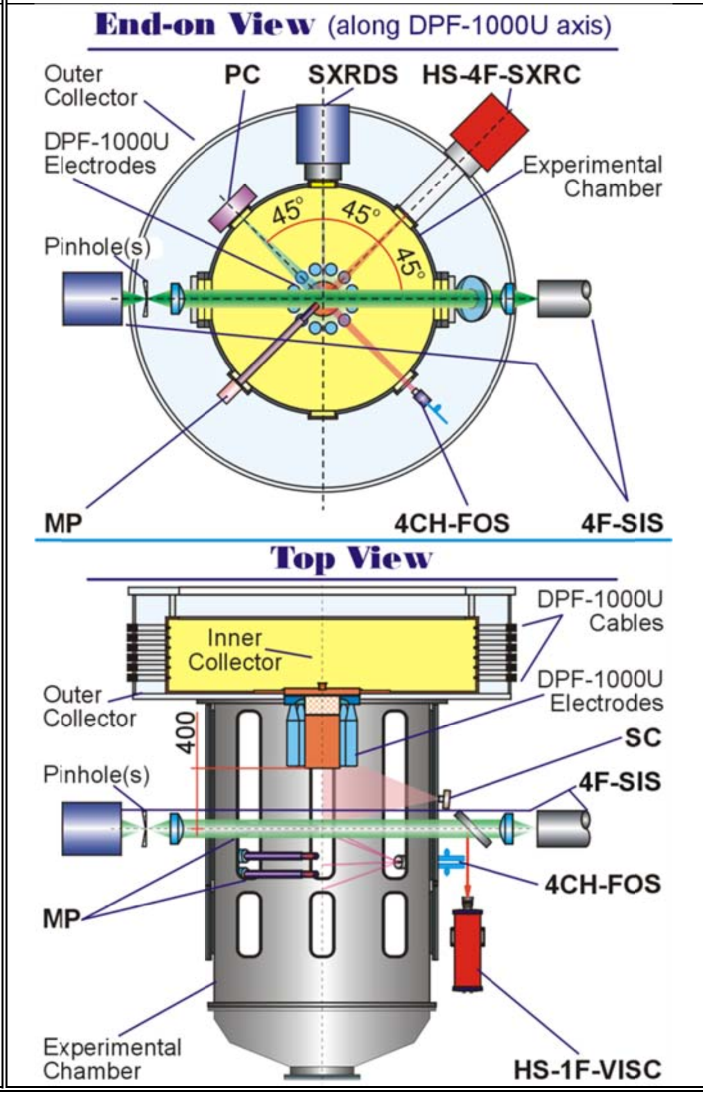

	Diagnostic Equipment Acronyms Description	
Acronym	**Full name and primary research use**	**Info on the page(s)**
PC	**P**inhole **C**amera; Applied for recording of time-integrated, soft X-ray images of plasma column.	
SXRDS	**S**oft **X**-**r**ay **D**etection **S**et; Applied for recording of radiation pulses emitted from plasma column in soft X-ray spectral range.	**9-10**
HS-4F-SXRC	**H**igh-**S**peed **F**our-**F**rame **S**oft **X**-**r**ay **C**amera; Applied for recording of time-resolved, soft X-ray images of plasma column.	**7-8**
16F-LIS	**S**ixteen-**F**rame **L**aser **I**nterferometry **S**ystem; Used to reconstruct the electron density distribution inside the plasma column (after processing).	**3-4**
4F-SIS	**F**our-**F**rame **S**chlieren **I**maging **S**ystem; Used to reconstruct the gradient of electron density distribution inside the plasma jets (after processing).	**5-6**
HS-1F-VISC	**H**igh-**S**peed **S**ingle-**F**rame UV/**VIS**/NIR **C**amera; Applied for time-resolved imaging of plasma jet flow in optical spectral ranges.	
MP	**M**agnetic **P**robes; used to reconstruct the radial distribution of the magnetic field in plasma and its surroundings.	
4CH-FOS	**F**our-**Ch**annel **FO S**ystem; Applied for estimation of plasma jet flow speed.	**11-12**
SC	**S**till **C**amera; Applied for time-integrated imaging of discharge & plasma flow.	

16F-LIS	Sixteen-Frame Laser Interferometry System

Design & Manufacturing or Integration/Assembling	
DPF-1000U Team, IPP&LM, Warsaw, POLAND	
Time of the first application of current version	March, 2010

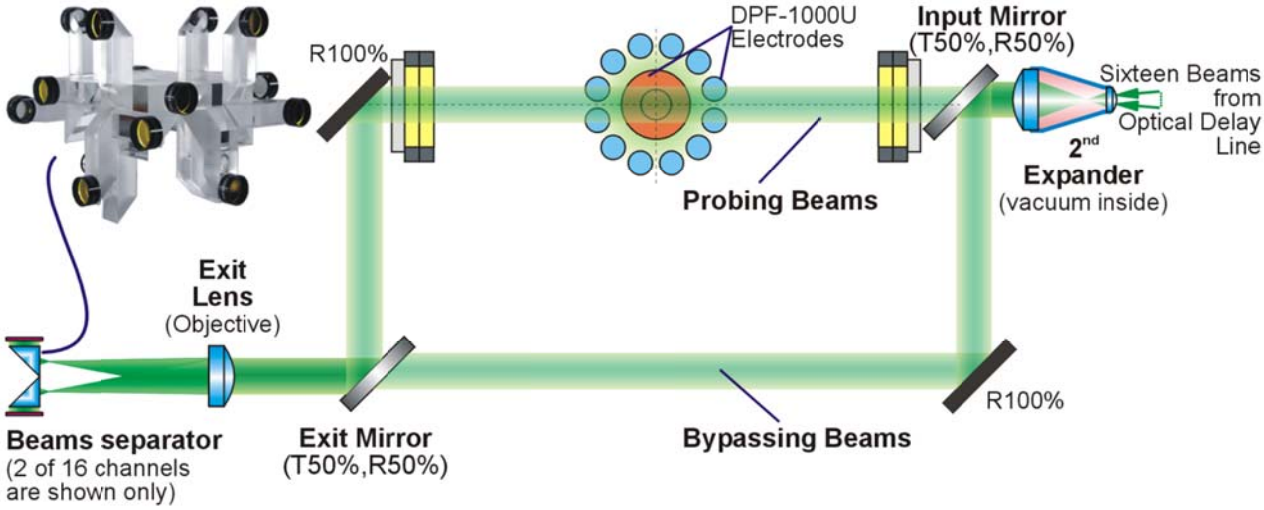

The simplified scheme of 16F-LIS;
In the left upper part the real view of 16-Channel Beams Separator is shown, in which one may distinguish right angle and rhomboid prisms as well as interference filters installed at the each of channel output.

Basic Info

The 16-Frame Laser Interferometry System uses the second harmonic of the Nd:YLF pulse laser (FWHM~1 ns, 527 nm, 500 mJ) as a bright and coherent radiation source. Besides laser, the system includes: the optical delay line that splits incoming laser beam on to 16 beams delayed to each other, high-aperture interferometer (Mach-Zehnder layout) and a custom designed beams separator followed by photographic plates set. The system is able to record sixteen consecutive interferometric images of plasma column during single discharge performed in the DPF-1000U device with millimeter spatial resolution and nanosecond temporal resolution.

More Info

The second harmonic of Q-switched Nd:YLF laser (FWHM~1 ns, 527 nm, 500 mJ) is applied as a radiation source for the 16-Frame Laser Interferometry System. Initially, to minimize the natural divergence of the output laser beam (diameter 12 mm), it is widened to a diameter of 60 mm.

The beam prepared in this way is directed to an optical delay line containing a series of fully reflective (R ~ 100%) and translucent (T ~ 50%) mirrors. Applied delay line topology ensures creation of sixteen, time and space separated beams. The time interval between each subsequent pair of beams is 10ns or (alternating) 20ns, giving a total delay between the first and sixteenth beams of 220ns. The bunch of 16 beams is directed at very small angles (in relation to the common optical axis of the system) to the second expander, where each beam is widened to a diameter of 150 mm.

Then, all the beams hit on the input mirror of the Mach-Zehnder (MZ) interferometer, where they are splitted into probing beams (passing through the device's chamber and plasma), and reference beams (bypassing the device's chamber). Each pair of beams (i.e. probing & corresponding bypassing beams) interfere with each other at the output mirror of the MZ interferometer. Obtained in this way interferometric images are conveyed onto surface of photographic plates by means of an exit lens (objective). In the focal plane of this objective, interference beams are of the smallest spatial size (spots) and are distributed evenly around the common optical axis of the system in the form of a matrix of four groups, each of which consists of four spots.

Due to the small size of the spots, the focal plane vicinity is the only place where it is possible to separate successive interference beams into recordable interferometric frames. In the first step, the propagation direction of the four groups of interference beams is redirected by four right angle prisms to directions approximately perpendicular to the common optical axis of the system (left, up, right and down). Then, the beams in each group are shifted by a certain constant distance in the direction away from the group axis, which allows to avoid their mutual overlapping during the final registration on the photographic plate. This is done by means of four identical rhomboid prisms permanently installed on the exit surface of each of the right angle prisms. Each of the sixteen beams coming out of the rhomboid prism must pass through its own narrowband interference filter, which allows for a strong reduction of the undesirable effect of the very intense plasma self-luminosity. Behind the described beam separator, there are four photographic plates (each for recording four interferometric frames), specially selected for optimal contrast and spatial resolution of the images taken.

Both the diameter of each probing beam and the total delay time between the first and the last beam allow the visualization of all interesting phases of the PF phenomenon (i.e. the radial compression phase, the pinch formation, the development of MHD instabilities and disintegration of the plasma column), during each single discharge carried out in the DPF-1000U device. Such a 16-frame visualization allows, after appropriate processing, to obtain the distributions of electron density inside the plasma column with millimeter spatial resolution and nanosecond time resolution (determined by the laser pulse FWHM).

Exemplary results taken during experimental campaign performed on DPF-1000U device

Plasma column filamentation recorded during its stagnation and disruption phases;
Initial pressure:0.8 Torr D_2; Gas-puff: 1bar (50%D_2+50%He); Time 0 corresponds to the first minimum of the dI/dt signal;
z = 0 corresponds to the face of the central electrode; Pinholes uncovered, radiation recording within full spectral range

The copper jet formation and propagation along the DPF-1000U device's axis;
Initial pressure:0.9 Torr D_2; Time 0 corresponds to the start of plasma jet creation;
z = 0 corresponds to the cone insert apex; Pinholes uncovered, radiation recording within full spectral range

Journal's (or other) paper with detailed technical description

E. Zielińska, M. Paduch, and M. Scholz, **Sixteen-frame interferometer for a study of a pinch dynamics in PF-1000 device**; *Contributions to Plasma Physics* (2011) **51,** 2-3:279-283

Official leaflet/datasheet

None

Five, most crucial and topical references

1. Kasperczuk A. *et al.*; **A plasma focus device as a metallic plasma jet generator;** *Laser and Particle Beams*, Volume 34, Issue 2, June 2016, pp. 356 – 361**;** DOI: https://doi.org/10.1017/S0263034616000215
2. Kubes P. *et al.*; **The influence of the nitrogen admixture on the evolution of a deuterium pinch column;** *Physics of Plasmas* **23**, 082704 (2016); https://doi.org/10.1063/1.4960825
3. Kubes P. *et al.*; **Filamentation in the pinched column of the dense plasma focus;** *Physics of Plasmas* 24, 032706 (2017); https://doi.org/10.1063/1.4978558
4. Kubes P. *et al.*; **Evolution of the Pinched Column During Hard X-ray and Neutron Emission in a Dense Plasma Focus;** *J Fusion Energy* **38,** 490–498 (2019). https://doi.org/10.1007/s10894-018-0194-x
5. Kubes P. *et al.*; **Characteristics of closed currents and magnetic fields outside the dense pinch column in a plasma focus discharge;** *Physics of Plasmas* **27**, 092702 (2020); https://doi.org/10.1063/5.0010249

Design & Manufacturing or Integration/Assembling	
DPF-1000U Team, IPP&LM, Warsaw, POLAND	
Time of the first application of current version	**March, 2010**

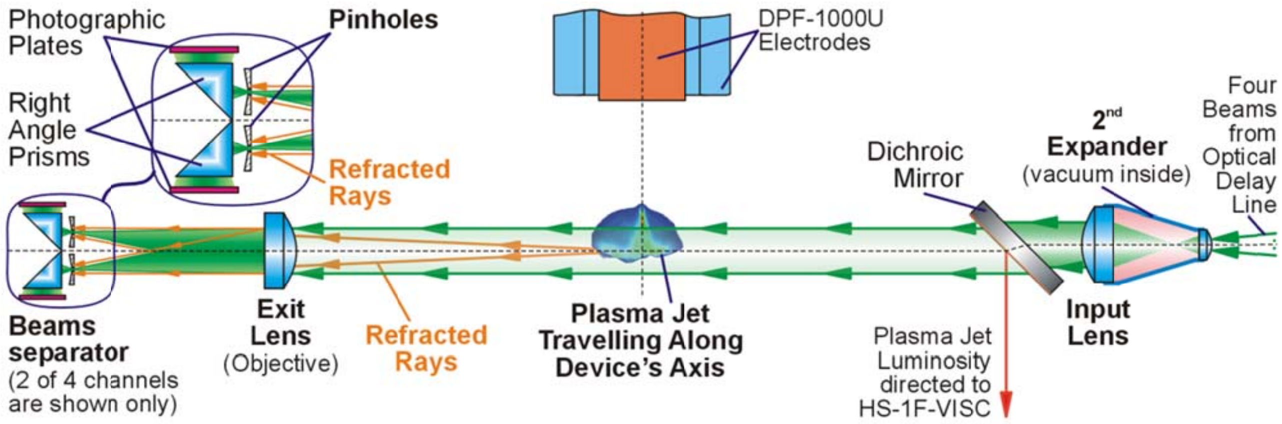

The simplified scheme of 4F-SIS applied to plasma jet propagation studies

Basic Info

The 4-Frame Schlieren Imaging System is based on the slightly modified Teopler layout (instead knife edge a pinhole(s) is applied). As a source of bright radiation for the system, a pulsed Nd:YLF laser operating with the second harmonic (FWHM ~ 1 ns, 527 nm, 500 mJ) is used. The four, delayed to each other, laser beams are freely selectable from the 16-channel optical delay line - the routinely dedicated to the laser interferometry system. The bunch of four beams pass through two lenses setup, between which plasma appears. Strictly in the focal plane of the system exit lens, the matrix of four pinholes is installed. Thanks to that, some part of rays refracted by plasma are blocked (definitely removed from final images). The unblocked part of each beam hits on the beams separator and finally is conveyed onto a surface of the four photographic plates. The system configured in this way is able to record four consecutive schlieren images of a plasma column or plasma jet with millimeter spatial resolution and nanosecond temporal resolution.

More Info

As with the laser interferometry system, the second harmonic of Q-switched Nd:YLF laser (FWHM~1 ns, 527 nm, 500 mJ) is applied as a radiation source for the 4-Frame Schlieren Imaging System. Initially, to minimize the natural divergence of the output laser beam (diameter 12 mm), it is widened to a diameter of 60 mm. The beam prepared in this way is directed to an optical delay line containing a series of fully reflective (R ~ 100%) and translucent (T ~ 50%) mirrors. Applied delay line topology ensures creation of sixteen, time and space separated beams. However, only any four beams can be selected for schlieren imaging purposes.

The bunch of 4 beams is directed at very small angles (in relation to the common optical axis) to the second expander. The expander output lens has a large aperture (220 mm dia.) and a long focal length. It widens each beam (up to a diameter of 200 mm) and collimates it accordingly. The collimated beams pass through the device's chamber and are then focused using an exit lens (objective) which has similar parameters (aperture, focal length) as the input lens.

In the focal plane of this objective, beams are of the smallest spatial size (spots) and are distributed evenly around the common optical axis of the system. The matrix of four pinholes is placed exactly in this place, and their spatial distribution must exactly match the position of these four spots. This is crucial to achieving the primary research purpose for which the system was built. The beams pass through the pinholes and hit the beam separator, which consists of four right angle prisms. The propagation direction of each beam is redirected to directions approximately perpendicular to the common optical axis of the system (left, up, right and down). Eventually, each beam passes by narrow band interference filter and is focused on its own photographic plate (one of the four) on which it is recorded.

If no object appears on the path of the collimated beams, the images recorded by the system will have the form of a more or less gray background with even distribution. The appearance of plasma in the space of collimated beams changes this state diametrically. Based on the relationships known from plasma physics and taking into account the wavelength of the laser used, it is possible to calculate the critical electron density, the value of which ($3.6 \ast 10^{21}$ cm^{-3}) exceeds by at least two orders of magnitude the maximum observed electron density during the PF phenomenon.

Thus, it can be said that in the case of the presented system we will always have to do with underdense plasma which behaves like a transparent, nonlinear refractive medium through which collimated beams are passed. If the beams move in the x-direction, then the refractive index gradients $\partial n/\partial y$ and $\partial n/\partial z$ refract some of the rays. When the refraction angle exceeds a predetermined value, the refracted rays are unable to hit the aperture (pinhole) area and are blocked by the opaque surroundings of the apertures. In result, a dark spots appear on the captured image. Taking into account the dependence of the plasma refractive index on its electron density and generalizing the above-described phenomena to all rays in the beam, it can be concluded that using the presented system, four schlieren images are obtained, in which electron density gradients greater than assumed are represented by dark zones mapped on a gray background.

To provide an identical line of sight for the schlieren imaging system and the high-speed, single-frame visible camera, a dichroic mirror was installed between the two lenses of the Toepler layout. This is obviously an undesirable component, although its use was necessary to achieve assumed objectives of plasma jet propagation studies.

Exemplary results taken during experimental campaign performed on DPF-1000U device

Plasma column filamentation recorded during its stagnation and disruption phases;
Initial pressure:0.8 Torr D_2; Gas-puff: 1bar (50%D_2+50%He); Time 0 corresponds to the first minimum of the dI/dt signal;
z = 0 corresponds to the face of the central electrode; Pinholes uncovered, radiation recording within full spectral range

The copper jet formation and propagation along the DPF-1000U device's axis;
Initial pressure:0.9 Torr D_2; Time 0 corresponds to the start of plasma jet creation;
z = 0 corresponds to the cone insert apex; Pinholes uncovered, radiation recording within full spectral range

Journal's (or other) paper with detailed technical description

None

Official leaflet/datasheet

None

Five, most crucial and topical references

1. Kasperczuk A. *et al.*; **A plasma focus device as a metallic plasma jet generator;** *Laser and Particle Beams*, Volume 34, Issue 2, June 2016, pp. 356 – 361**;** DOI: https://doi.org/10.1017/S0263034616000215
2. Kubes P. *et al.*; **The influence of the nitrogen admixture on the evolution of a deuterium pinch column;** *Physics of Plasmas* **23**, 082704 (2016); https://doi.org/10.1063/1.4960825
3. Kubes P. *et al.*; **Filamentation in the pinched column of the dense plasma focus;** *Physics of Plasmas* 24, 032706 (2017); https://doi.org/10.1063/1.4978558
4. Kubes P. *et al.*; **Evolution of the Pinched Column During Hard X-ray and Neutron Emission in a Dense Plasma Focus;** *J Fusion Energy* **38,** 490–498 (2019). https://doi.org/10.1007/s10894-018-0194-x
5. Kubes P. *et al.*; **Characteristics of closed currents and magnetic fields outside the dense pinch column in a plasma focus discharge;** *Physics of Plasmas* **27**, 092702 (2020); https://doi.org/10.1063/5.0010249

HS-4F-SXRC	High-Speed Four-Frame Soft X-ray Camera	
	Design & Manufacturing or Integration/Assembling	
	ACS Laboratory, ACS Ltd., Warsaw, POLAND	
	Time of the first application of current version	**September, 2015**

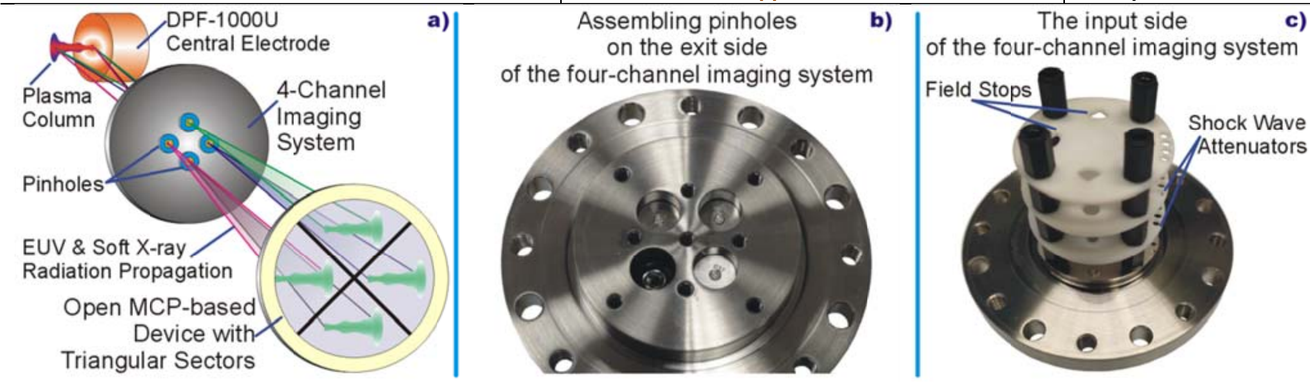

The HS-4F-SXRC;
a) The principle of plasma column visualization; b),c) Some details of the four-channel imaging system

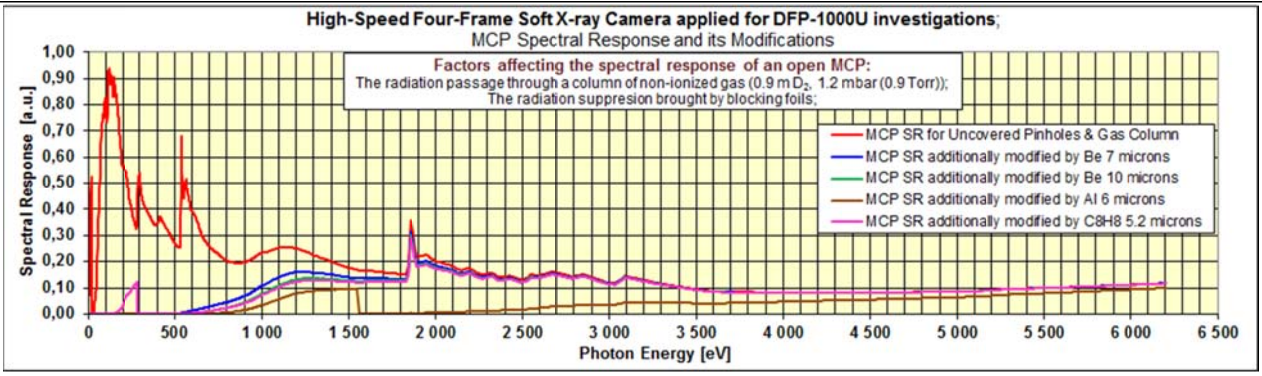

The MCP spectral response and its modifications, which can be introduced through the use of various blocking foils

Basic Info

The High-Speed, Four-Frame Soft X-ray Camera (HS-4F-SXRC) is able to record four images of plasma column in extreme UV and soft X-ray spectral ranges (10÷6200 eV) with nanosecond temporal and sub-millimeter spatial resolutions.

More Info

In camera a gateable, open MCP-based device acts as the primary detector, fast shutter and radiation amplifier. This device consists of MCP (microchannel plate) and phosphor screen, which are divided into four electrically independent (triangular) sectors. Each sector can be gated by only one (positive) electrical pulse with amplitude of 5÷6 kV, applied between a phosphor screen and an input side of the MCP (which is connected to a common ground).

For image registration purposes, an open MCP-based device acts as a part of well-known *"camera obscura"* or "*pinhole camera*" layout and in consequence must cooperate with four-channel imaging system containing a set of four interchangeable pinholes (made of platinum-iridium), the useful diameters of which may be in the range 30÷150 microns.

Due to a very efficient differential pumping system connected to the camera, pinholes can be full open (not covered by blocking foils). Despite the constant leak of gas from the DPF device's chamber, the vacuum conditions ($<5 * 10^{-3}$ Pa) necessary for proper operation of the open MCP are maintained. This in turn means that apart usually recorded soft X-ray radiation, the camera is also able to record low-energy quanta emitted in the extreme UV spectral range (EUV, 10÷124 eV; 10÷124 nm). However, if necessary - in order to limit spectral range of recorded radiation, a suitable blocking foil can be applied. In such case, a vacuum tight foil holder is mounted just above pinhole. Alike in a case of pinhole, every recording channel can be equipped with its own, replaceable blocking foil.

The image information transferred by the phosphor screen radiance is captured by means of final image detector, whose role plays the high resolution CCD array. An analogue signal outgoing from CCD is digitized and acquired in on-board mounted memory (2048x2048x16 bit) and then can be durably saved on a system controller's hard disk. An optical coupling between phosphor screen and CCD matrix is ensured by means of F/1.4 relay lens.

The camera works routinely with an exposure time of no more than 1.8 ns. The limiting spatial resolution (achieved at this exposure time) is not worse than 1 lp/mm (related to the central plane of the DPF-1000U device), which means that the two singularities of the plasma column about 500 microns apart can be correctly reconstructed.

The four-point spring mounting of the camera design along with three precision adjuster screw allow performing precise angular alignment of the camera's line-of-sight within ± 3° pitch/yaw. Such kind change of the camera's field of vision can be done even under required vacuum conditions inside it.

Owing to: battery powering, galvanic separation, electromagnetically tight housings and communication with outside via optical pulses only, the camera has high immunity against electromagnetic interference usually accompanying high energy/power experiments.

Exemplary results taken during different experimental campaigns performed on DPF-1000U device

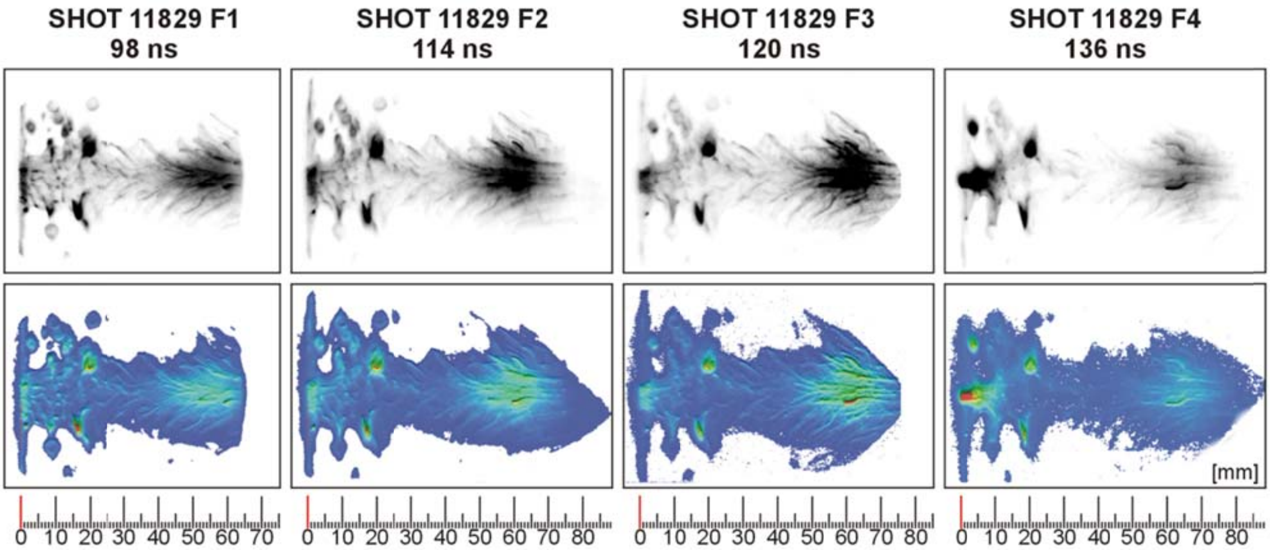

Plasma column filamentation recorded during its stagnation and disruption phases;
Initial pressure:0.8 Torr D_2; Gas-puff: 1bar (50%D_2+50%He); Time 0 corresponds to the first minimum of the dI/dt signal;
z = 0 corresponds to the face of the central electrode; Pinholes uncovered, radiation recording within full spectral range

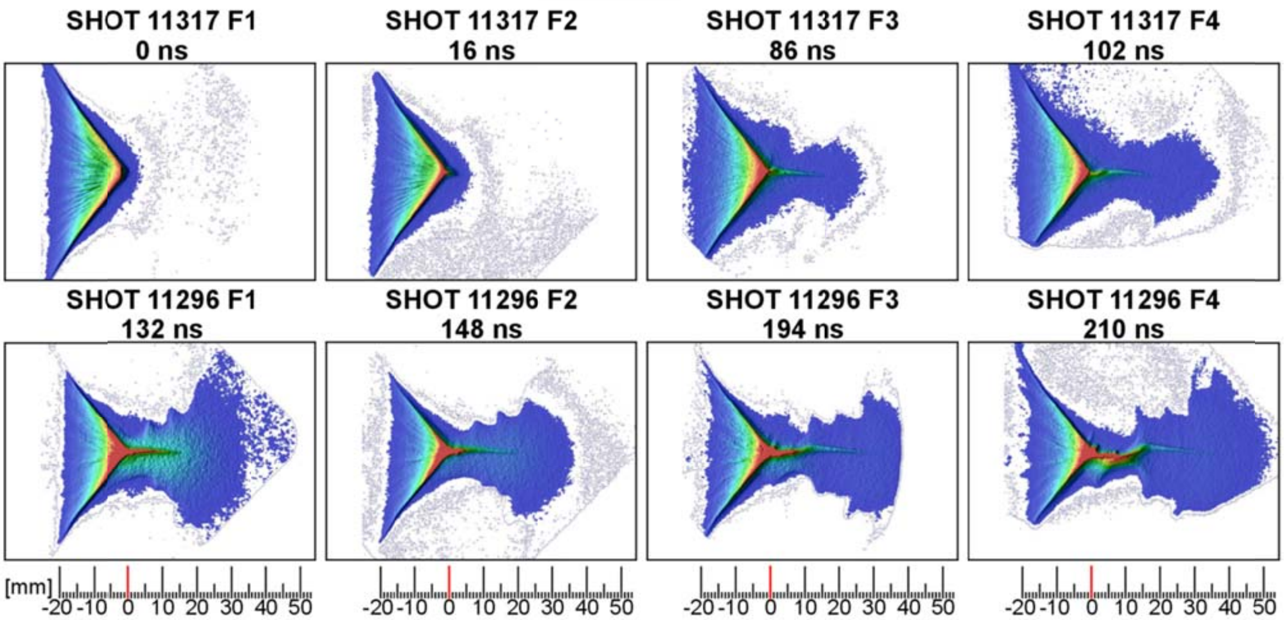

The copper jet formation and propagation along the DPF-1000U device's axis;
Initial pressure:0.9 Torr D_2; Time 0 corresponds to the start of plasma jet creation;
z = 0 corresponds to the cone insert apex; Pinholes uncovered, radiation recording within full spectral range

Journal's (or other) paper with detailed technical description

None

Official leaflet/datasheet

None

Five, most crucial and topical references

1. Kasperczuk A. *et al.*; **A plasma focus device as a metallic plasma jet generator;** *Laser and Particle Beams*, Volume 34, Issue 2, June 2016, pp. 356 – 361**;** DOI: https://doi.org/10.1017/S0263034616000215
2. Kubes P. *et al.*; **The influence of the nitrogen admixture on the evolution of a deuterium pinch column;** *Physics of Plasmas* **23**, 082704 (2016); https://doi.org/10.1063/1.4960825
3. Kubes P. *et al.*; **Filamentation in the pinched column of the dense plasma focus;** *Physics of Plasmas* 24, 032706 (2017); https://doi.org/10.1063/1.4978558
4. Kubes P. *et al.*; **Evolution of the Pinched Column During Hard X-ray and Neutron Emission in a Dense Plasma Focus;** *J Fusion Energy* **38,** 490–498 (2019). https://doi.org/10.1007/s10894-018-0194-x
5. Kubes P. *et al.*; **Characteristics of closed currents and magnetic fields outside the dense pinch column in a plasma focus discharge;** *Physics of Plasmas* **27**, 092702 (2020); https://doi.org/10.1063/5.0010249

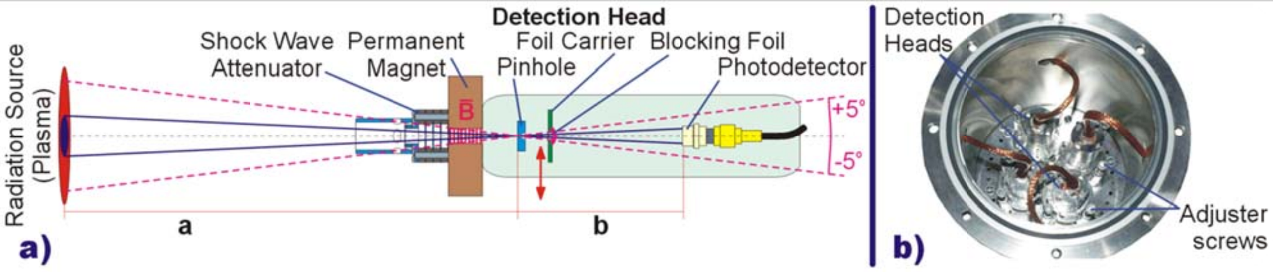

a) the pinhole camera layout applied to the DH's design and location of the head's most important elements; b) the four detection heads installed inside the vacuum chamber of the SXRDS

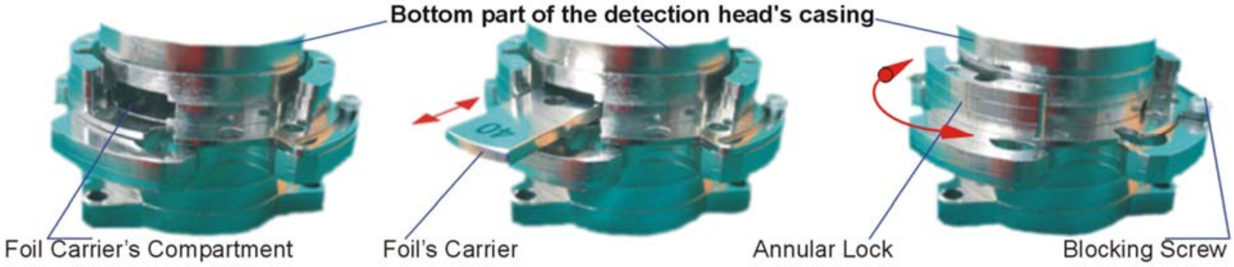

The detection head elements enabling replacement of the blocking foil and ensuring its reproducible position with reference to the detection head's line-of-sight

Basic Info

The Soft X-ray Detection Set (SXRDS) includes four independent detection heads that are able to record the radiation pulses emitted from plasma column in soft X-ray spectral range (~0.5÷12 keV) with sub-nanosecond temporal resolution.

In the basic operation mode, the SXRDS records the time-resolved and space-resolved radiation from up to four different areas of the plasma column. SXRDS can also be configured for measurements with temporal and spectral resolution, in which the radiation emitted from the same area(s) of the plasma column is captured.

More Info

Up to four detection heads (DHs) can be installed in the SXRDS vacuum chamber. Each individual DH may be based on different photodetectors (e.g. P-I-N silicon diode, GaAs, diamond). The most characteristic feature of the DH is the use of a pinhole in front of the photodetector.

This unconventional arrangement is certainly much more useful compared to the standard configuration where the photodetector collects photons from the 2π solid angle. The use of a pinhole camera layout in the DH design ensures precise definition of the DH's field-of-vision and possibility of its proper location on the interesting part of the plasma column only.

Assuming that the distance "a" between the pinhole and the radiation source is constant (see diagram above), appropriate field of vision can be selected by: firstly, change of distance "b" between pinhole and detector surface, secondly, replacing the photodetector to another one with a smaller or larger active area. Due to a modular design of the DH, change of distance "b" is practicable by adding or removing head's spacers.

Application of pinholes with low aperture (tens of microns) has several additional advantages, namely - it allows avoiding overloading of the photodetector and exclude the recording of undesirable, parasitic radiation reflected from elements of the device chamber. Moreover, it also improves a blocking foil immunity (typically a few microns thick) against very strong shock waves accompanying the PF discharge.

To further improve that immunity, the DH can be equipped with a detachable shock wave attenuator. It consists of input cylinder followed by five diaphragms with a gradually decreasing diameter. Six permanent magnets are installed on the underside of the SXRDS carrier plate. Their magnetic field is (more or less) perpendicular to each of the DH's line-of-sight, and their magnetic induction reaches a value of about 0.46 T. This, in conjunction with shock wave attenuator's components, protects both the blocking foils and the photodetector active surface against strong fluxes of charged particles emitted in the final stages of the PF phenomenon.

In the design solution used in the DH, the blocking foil is mounted on a standard carrier, which can be replaced with another one in a fairly simple and fast way. The blocking foil's proper position across line-of-sight (accuracy ±0.1 mm) is secured by additional elements applied to the DH's design (see diagram above). It should be underlined that the foil carrier's replacement does not affect on earlier adjusted line-of-sight. Moreover, due to cut-off valve and vacuum bypass accompanied the SXRDS vacuum chamber such replacement can be done without venting the DPF-1000U device's chamber.

Each DH has its own two-point spring mounting and two precision adjuster screws with differential thread (pitch equal to 0.1 mm). It allows performing very fine angular alignment of the head's line-of-sight within ± 5° pitch/yaw. The set of the custom-designed appliances/procedures have been prepared for the DHs alignment/adjustment purposes. This secures the accuracy better than ±0.5 mm in the location of the individual line of sight on the desired part of the plasma column.

Exemplary results taken during experimental campaign performed on DPF-1000U device

Photodetector Si P-I-N S9055 type

During the experiments conducted from June 2012 to the present day, the four DHs used in SXRDS were most often equipped with a silicon P-I-N photodiode S9055 (HAMAMATSU). In fact, this photodetector (PD) was then the workhorse of the discussed diagnostics.

To obtain the shortest possible response time of this PD, it was attached to the SMA bulkhead connector. This largely eliminates the interconnection inductance and provides very good matching conditions for a 50 Ω transmission line. Bandwidth and response time tests of the PD were performed with a femtosecond laser used as a delta-function light source. The obtained results showed that in such prepared PD the bandwidth is equal to 4 GHz, the response time does not exceed 220 ps and the limiting time resolution is not worse than 200 ps.

The calculated PD's spectral response and its modifications brought by different blocking foil are shown below. In described experiment, all the detection heads were equipped with pinhole (80 microns dia.) that were blocked by a beryllium foil (10 microns thick).

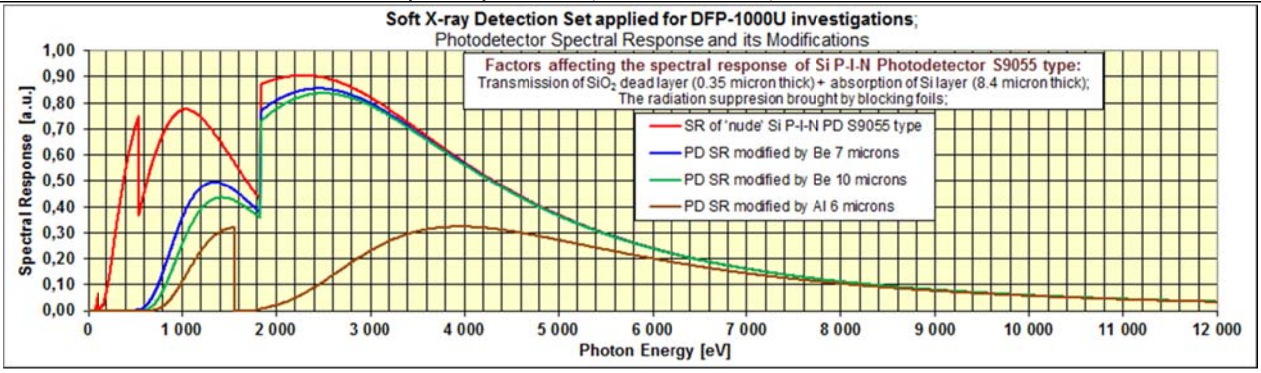

The PD's spectral response and its modifications, which are introduced through the use of various blocking foils

The photodetector's active area (200 microns dia.) along with the applied pinhole camera parameters (a=1064 mm, b=6.9 mm) ensured field-of-vision diameter of about 31 mm (in relation to the central, horizontal plane of the PF device) for all the detection heads employed in the SXRDS. The detailed location of axial points and field-of-visions for individual line-of-sight are shown in the right part of the chart below.

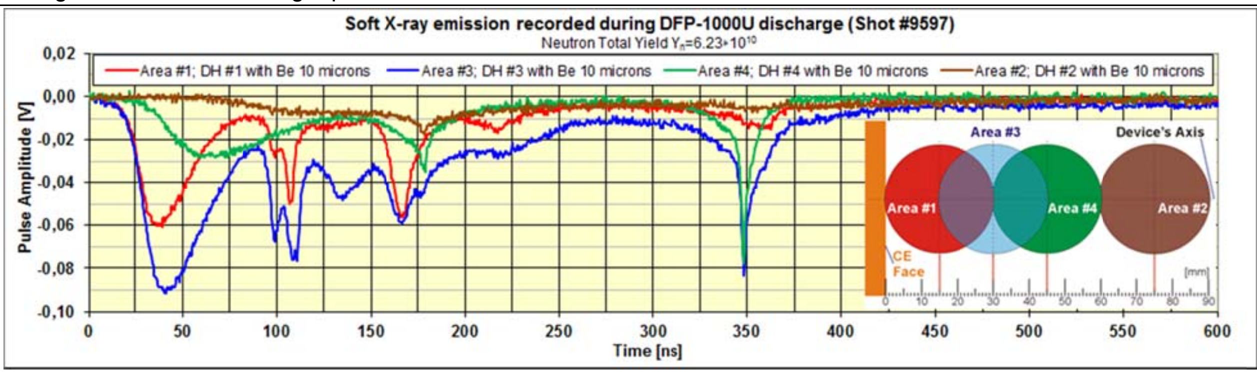

Soft X-ray pulses recorded from four areas of the plasma column;
The schematic position of these areas in relation to the device's CE and axis is shown in the right part of the chart;
The colors of the waveforms correspond to the colors of the areas from which radiation is captured;
Time 0 corresponds to the start of soft X-ray emission; z = 0 corresponds to the face of the central electrode;

Journal's (or other) paper with detailed technical description

None

Official leaflet/datasheet

None

Five, most crucial and topical references

1. W Surała *et al.*; **Recent measurements of soft X-ray emission from the DPF-1000U facility;** *Nukleonika* 2015, Vol. 60, No. 2 pp.303-308; DOI: 10.1515/nuka-2015-0055
2. M J Sadowski *et al.*; **Soft x-ray studies of plasma-focus pinch structures in PF-1000U experiments;** 2015 *Plasma Sources Sci. Technol.* 24 055003; https://doi.org/10.1088/0963-0252/24/5/055003
3. Kubes P. *et al.*; **Influence of the Al wire placed in the anode axis on the transformation of the deuterium plasma column in the plasma focus discharge;** *Physics of Plasmas* 23, 062702 (2016); https://doi.org/10.1063/1.4953569
4. Kubes P. *et al.*; **Filamentation in the pinched column of the dense plasma focus;** *Physics of Plasmas* 24, 032706 (2017); https://doi.org/10.1063/1.4978558
5. D R Zaloga *et al*.; **Influence of gas conditions on electron temperature inside a pinch column of plasma-focus discharge;** 2018 *J. Phys.: Conf. Ser.* **959** 012003; https://doi.org/10.1088/1742-6596/959/1/012003

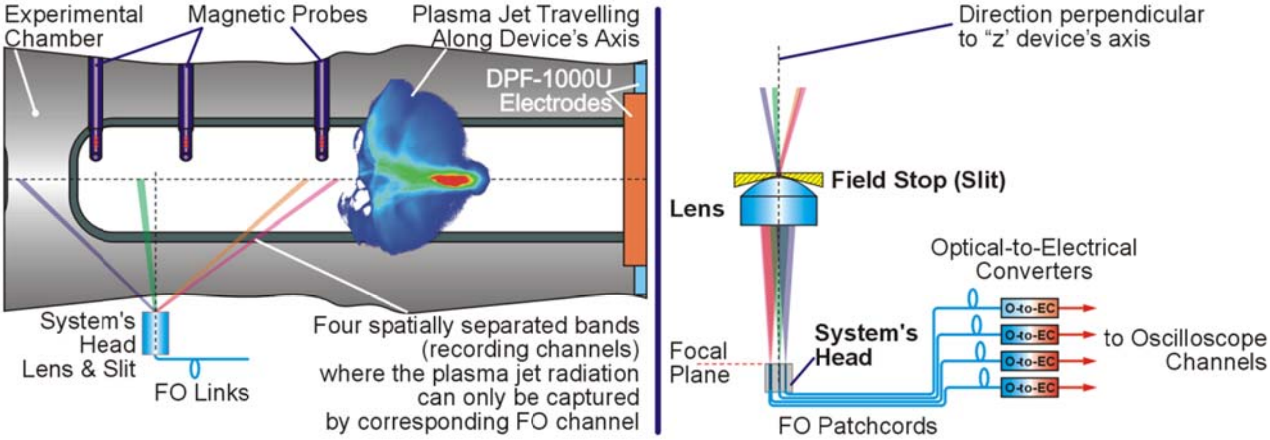

The simplified (out of scale) scheme of 4CH-FOS and its principle of operation

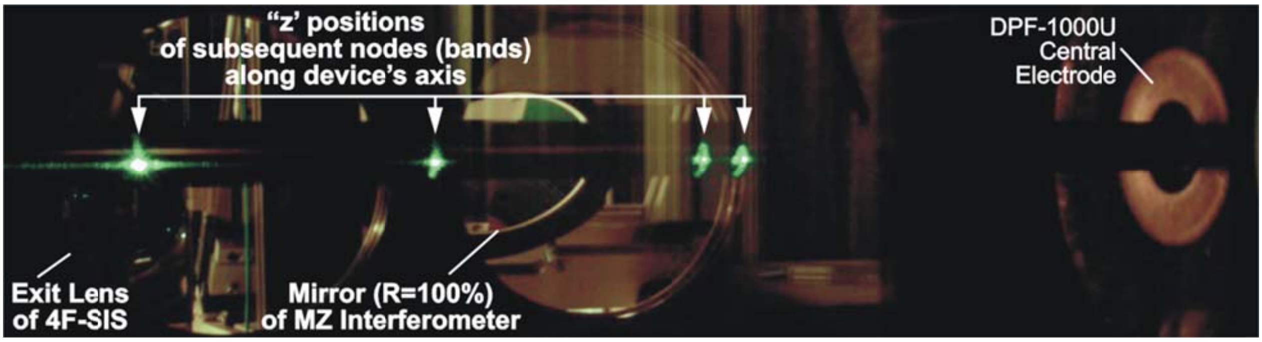

Alignment procedure of 4CH-FOS;
The spots of the laser beams mapped on the surface of the bar temporarily installed along the device's axis

Basic Info

The Four-Channel Fiber Optic System (4CH-FOS) is used to estimate the velocity of the plasma jet traveling along the central "z" axis of the device. In particular, it concerns the space outside the standard diagnostic field-of-vision – at distances from the CE face above 130 mm. The idea is to record the plasma radiation (approximately proportional to the square of the electron density) in four separate, narrow regions (bands) through which the plasma jet passes sequentially. The intervals between the four pulses recorded by the oscilloscope - corresponding to the plasma passage through successive bands, along with the known distances between them (in reference to the central axis of the device), allow to estimate the speed of the plasma jet.

More Info

The key element of the four-channel fiber system (4CH-FOS) is the FO head containing four multimode fibers (125/65 micron clad/core, NA - 0.22), in a serial, close packing with some spaces to each other. The stability of the position of the individual fibers is ensured by epoxy potting. The head face is polished to obtain the optical quality of the ends of the optical fibers. Four short patchcords are led out from the back surface of the head. They are equipped with STII FO connectors that along with bulkhead connectors can be used for further extension of FO links.

The front face of the head (and the ends of the optical fibers at the same time) are placed exactly in the focal plane of the lens of the system. If a radiant flux (e.g. from a bright LED or portable laser) is introduced to all fibers from the side of STII connectors (usually a FO signal splitter is used for this purpose), then at the output of the fibers there will be created four bunches of rays limited by a conical surface, resulting from the numerical aperture of the fibers.

Bunches of rays passing through the lens (which in this case acts as a collimator) are transformed into more or less collimated beams. The angular deviation of each of the collimated beams (in relation to the optical axis of the lens) is related to the position of the corresponding optical fiber. The greater the distance between the fiber and the optical axis, the greater the deflection of the collimated beam.

Exactly on the exit surface of the lens is installed narrow slit (i.e. field stop) which direction is exactly perpendicular to the row of FO ends in the system head. It is obvious, that part of each collimated beam is blocked by the opaque surroundings of the slit. As a result, one of the dimensions of the beams (parallel to the slit) will be significantly narrowed. Thanks to that the outgoing beams will propagate in space as a narrow bands. The position where each band crosses the "z" axis of the device creates a virtual node, from which area the radiation emitted by the plasma jet is captured (during actual measurement).

To visualize the actual position of each virtual node, an additional element (e.g. a rod) is usually (and of course temporarily) installed along the "z" axis of the device. The spots of the bands mapped on the surface of the bar allow for precise measurement of their coordinates along the "z" axis (see the diagram above). The design of the discussed system enables the head to move in the direction perpendicular to the optical axis of the lens. As a result, the location of the nodes can be freely set (in a certain, allowed range).

During the discharge performed on the DPF-1000U device, plasma radiation - approximately proportional to the square of the electron density, is captured in the area of each node and hits the corresponding optical fiber located in the system's head. All optical signals propagate further along the FO links and eventually reach the optical-to-electrical converters, where they are converted into corresponding electrical signals (in analog mode), which are then recorded by a four-channel oscilloscope.

Based on the data stored in the oscilloscope's memory, a time analysis of the recorded waveform is performed, consisting in measuring the intervals between successively recorded pulses - corresponding to the passage of plasma through successive nodes. These intervals are measured at the leading edges of the pulses at an amplitude of half the maximum value. The obtained results are corrected by the values resulting from: differences in the quantum flight time from the nodes to the front surface of the lens of the system and delays in optical links (measured by the reflectometric method).

The interval measurement error is estimated at ±1 ns and is mainly due to the sampling frequency used in the oscilloscope (1 GS/s), while the error in measuring the distance between nodes is within ±0.5 mm. Taking the above values as a basis, it can be calculated that the total error in estimating the plasma jet velocity does not exceed 1.5%.

Exemplary results taken during experimental campaign performed on DPF-1000U device

The PD's spectral response and its modifications, which are introduced through the use of various blocking foils

Soft X-ray pulses recorded from four areas of the plasma column;
The schematic position of these areas in relation to the device's CE and axis is shown in the right part of the chart;
The colors of the waveforms correspond to the colors of the areas from which radiation is captured;
Time 0 corresponds to the start of soft X-ray emission; z = 0 corresponds to the face of the central electrode;

Journal's (or other) paper with detailed technical description

None

Official leaflet/datasheet

None

Five, most crucial and topical references

1. V. I. Krauz *et al.*; **Generation of compact plasma objects in plasma focus discharge;** EPL, **129** (2020) 15003**;** DOI: 10.1209/0295-5075/129/15003